

Article

Evaluation of Supramolecular Gel Properties and Its Application in Drilling Fluid Plugging

Xiaoyong Du ¹, Shaobo Feng ¹, Haiying Lu ¹, Yingrui Bai ^{2,*}  and Zhiqiang Lv ¹¹ PetroChina Tarim Oilfield Company, Korla 841000, China² School of Petroleum Engineering, China University of Petroleum (East China), Qingdao 266580, China

* Correspondence: smart-byron@163.com

Abstract: Supramolecular gels are physically cross-linked hydrogels formed by non-covalent interactions. The synthesis, structure optimization, property regulation, and application expansion of supramolecular gels has gradually become the research hotspot in the field of gel materials. According to the non-covalent interactions such as hydrophobic association and hydrogen bonding, the supramolecular gel prepared in this study has excellent rheological properties and adaptive filling and plugging properties, and can be used in the field of drilling fluid plugging. In this paper, the microstructure, rheological properties, temperature resistance, and plugging properties of supramolecular gels were studied and characterized in detail. The experimental findings demonstrated that when the strain was less than 10%, the supramolecular gel displayed an excellent linear viscoelastic region. The increase in strain weakens the rheological properties of supramolecular gel and reduces the elastic modulus of supramolecular gel to a certain extent. The supramolecular gel still had a neat three-dimensional reticular structure after curing at high temperatures, and the network of each layer was closely connected. Its extensibility and tensile properties were good, and it had excellent temperature resistance and mechanical strength. The supramolecular gel had excellent tensile and compressive properties and good deformation recovery properties. When the elongation of the supramolecular gel reached 300%, the tensile stress was 2.33 MPa. When the compression ratio of supramolecular gel was 91.2%, the compressive stress could reach 4.78 MPa. The supramolecular gel could show an excellent plugging effect on complex loss layers with different fracture pore sizes, the plugging success rate could reach more than 90%, and the plugging layer could withstand 6.3 MPa external pressure. The smart plugging fluid prepared with supramolecular gel material could quickly form a fine barrier layer on the rock surface of the reservoir. It could effectively isolate drilling fluid from entering the reservoir and reduce the adverse effects, such as permeability reduction caused by drilling fluid entering the reservoir, so as to achieve the purpose of reservoir protection.

Keywords: supramolecular gel; non-covalent effect; rheological mechanical properties; plugging performance; drilling fluid plugging



Citation: Du, X.; Feng, S.; Lu, H.; Bai, Y.; Lv, Z. Evaluation of Supramolecular Gel Properties and Its Application in Drilling Fluid Plugging. *Processes* **2023**, *11*, 2749. <https://doi.org/10.3390/pr11092749>

Academic Editor: Sara Liparoti

Received: 23 August 2023

Revised: 4 September 2023

Accepted: 11 September 2023

Published: 14 September 2023



Copyright: © 2023 by the authors. Licensee MDPI, Basel, Switzerland. This article is an open access article distributed under the terms and conditions of the Creative Commons Attribution (CC BY) license (<https://creativecommons.org/licenses/by/4.0/>).

1. Introduction

Hydrogel is a kind of material that can form a three-dimensional network structure using free polymerization of polymers [1]. It contains a lot of water inside and is a soft substance between liquid and solid. Hydrogels can be prepared from a variety of raw materials, including polymer monomer materials, polymer materials, or a mixture of polymer monomer and polymer [2]. By changing the cross-linking mode of hydrogel, the cross-linking degree can be controlled, and the equilibrium swelling rate of hydrogel can be affected [3]. Although hydrogels can absorb large amounts of water in solutions of different pH, they can still maintain a certain form without dissolving [4]. As a kind of polymer soft material widely used and simple to prepare, the hydrogel can maintain its shape and size under the action of external force.

Hydrogels generally form the network structure of hydrogels via chemical cross-linking, physical cross-linking, and chemic-physical cross-linking [5,6]. Physically cross-linked hydrogels mainly form physical cross-linking networks via hydrogen bonds between molecular chains, static electricity, host-guest, hydrophobic interaction, and entanglement of molecular chains [7,8]. The physical cross-linking network of hydrogel was reversible under certain conditions, which broadened its range of applications [9]. Chemical cross-linked hydrogels form a chemical cross-linking network via chemical cross-linking points [10]. The chemical cross-linking network has high strength and toughness; once the chemical network is destroyed, it cannot be self-repaired under any conditions.

Dual network (DN) hydrogels have caused a great sensation as soon as they were proposed [11]. The double-network gel consists of most of the water and a small amount of polymer to form a double-network structure [12]. It not only has high strength and toughness but also is not consistent with the common hydrogel strengthening and toughening mechanism [13]. By inserting Fe^{3+} to interact with COOH and controlling the amount of acrylic acid in the hydrogel, Chen et al. enable the hydrogel to have high strength and toughness as well as fatigue resistance and quick self-healing [14,15]. With the deep application of hydrogels in various fields, higher and more stringent requirements have been put forward for the comprehensive performance of hydrogels, including the versatility of hydrogels and stable mechanical properties under various extreme conditions and strains. Li et al. created a three-network hydrogel with high strength, self-recovery, and high conductivity to make a robust strain sensor [16].

Recently, the new nanocomposite hydrogels have become the focus of the majority of researchers, with strong mechanical properties, high thermal stability, and so on [17]. Nanomaterials are included in the hydrogel system as physical cross-linking sites by specialists and academics from home and abroad. It may effectively raise the cross-linking degree of the hydrogel as well as the entanglement degree of the gel's molecular chain [18]. Yang et al. prepared polyacrylamide/lithium saponite nano-hydrogel by in situ free radical polymerization [19]. Under the best experimental conditions, the gel has more remarkable mechanical properties than the conventional gel. Gu et al. designed a polyacrylic hydrogel without adding chemical or physical cross-linking points, which can show ultra-high electrical conductivity [20]. The hybrid hydrogel may also fully heal on its own. In order to prevent the development and spread of fractures, nanocomposite hydrogel can efficiently disperse energy. This helps to enhance the mechanical characteristics of the hydrogel.

It is believed that the interpenetrating network structure is a useful technique for enhancing the mechanical characteristics of hydrogels [21]. One cross-linked polymer network is present in the hydrogel, while the other is still linear. Linear polymers are bonded to cross-linked polymer networks by van der Waals forces, electrostatic interactions, hydrogen bonding, hydrophobic association, or a combination of these interactions [22]. Wahid et al. prepared semi-interpenetrating network hydrogels using a chitosan network via cross-linked bacterial cellulose by introducing hydrogen bonding [23]. Compared to gel made from pure cellulose and chitosan, this gel exhibits superior mechanical and bactericidal capabilities. Zhu et al. used interpenetrating sodium carboxymethyl cellulose microspheres and polyacrylamide networks to form an ionic conducting hydrogel with remarkable mechanical strength, rapid response, large deformation, and stable cycling performance [24].

Hydrophobic association hydrogels refer to hydrophobic groups on hydrophilic macromolecular chains, which are aggregated via hydrophobic interaction [25]. Hydrophobic association between or within macromolecular chains forms physically cross-linked network hydrogels mainly used for intermolecular association. Tuncaboylu et al. copolymerized octadecyl methacrylate (C_{18}) and dodecyl acrylate (C_{22}) with acrylamide in sodium dodecyl sulfate by micellar copolymerization [26]. Via strong hydrophobic association, the gel had self-healing properties and high toughness. Chen et al. prepared a series of multi-stage cross-linked ionic hydrogels containing hydrophobic ionic liquids by cross-linking the hy-

drophobic ionic liquid with the crystalline fluorinated copolymer [27]. This ionic hydrogel had the characteristics of being non-volatile, transparent, stretchable, and sensitive.

Supramolecular gels have prospective uses in a variety of sectors recently, including medicine, biology, electronic engineering, and others [28]. Unlike traditional covalently bonded high molecular gels, supramolecular gels are mainly self-assembled by non-covalent bond interactions, which have reversible structure and high performance [29]. At present, the problem of good leakage has become particularly prominent, especially the problem of malignant leakage in complex drilling engineering [30,31]. The conventional hydrogel used for plugging has achieved good results in dealing with small and medium fractures and leakage of permeable drilling fluid. However, for large fractures or fracture-hole drilling fluid leakage, the adaptability of conventional gel and its plugging methods is relatively poor [32]. Jiang et al. developed a broad-spectrum supramolecular gel system with high strength and elasticity according to the theory and method of supramolecular chemistry [33]. In a controlled time, gels with certain strength could be formed in the loss layer and enter the formation pores or fractures to plug the loss layer.

The supramolecular gel can be used in the field of drilling fluid plugging because of its adaptable filling and plugging performance, great rheological and mechanical qualities, and superior mechanical properties. Based on this, supramolecular gels' microstructure, rheological characteristics, temperature resistance, and plugging characteristics were carefully examined and described. Excellent mechanical and plugging qualities of the supramolecular gel created in this work will lead to new applications for hydrogel in oil and gas drilling and production engineering.

2. Experiment

2.1. Synthesis of Supramolecular Gels

In this study, acrylamide (AM) is the main chain monomer, 2-acrylamido-2-methylpropanesulfonic acid (AMPS) is the monomer with high thermal resistance, and lauryl methacrylate (LMA) is the hydrophobic monomer. Meanwhile, sodium alginate (SSA), styrene monomer (SM) surfactant sodium lauryl sulfate (SDS), initiator potassium persulfate (KPS), and promoter sodium chloride (NaCl) were added to the deionized water. An inert atmosphere (nitrogen, 99.8%) was used to quickly degas the mixture after it had been agitated for an hour. Finally, the mixture was loaded into an airtight reactor and placed into an oven at 60 °C for 4 h. After a sufficient reaction, the homogenized solution was subjected to free radical polymerization at 300 r/min to prepare the supramolecular gel. Detailed preparative materials and mass concentrations are shown in Table 1.

Table 1. Supplies and dose for preparing supramolecular gel.

Material	AM	AMPS	SDS	NaCl	LMA	SSA	KPS	SM	Deionized Water
Dosage, g	100.0	10.0	30.0	20.0	10.0	3.0	3.0	1.0	323

2.2. Characterization of Microstructure

To create the freeze-dried supramolecular gel, the obtained supramolecular gel was first freeze-dried in liquid nitrogen at 50 °C and 30×10^{-3} mbar pressure for 48 h. The freeze-dried supramolecular gel was then carefully broken by injecting it into liquid nitrogen, placed on an aluminum root, and coated with a small coating of gold for scanning before being described by Hitachi S-4700 field emission scanning electron microscope (SEM) at 10 kV [34].

2.3. Rheological Properties Test

The HAAKE MARS 60 rheometer was used to describe the rheological features of supramolecular gel samples. The flat plate rotor utilized in the experiment was a P35/Ti type with a 35 mm rotor diameter [34]. First, stress scanning was used to identify the linear viscoelastic area of the supramolecular gel ($\gamma = 0.1\text{--}1000\%$). Secondly, angular

frequency (0–100 rad/s) scanning was performed on the supramolecular gel samples at fixed strain ($\gamma = 1\%$) to determine the energy storage modulus (G') and loss modulus (G'') of the supramolecular gels. Finally, the rheological properties of the supramolecular gels were verified by performing variable temperature (25–130 °C) scanning tests on the supramolecular gels at a fixed strain ($\gamma = 1\%$) and a constant shear rate ($\omega = 10$ rad/s) [34].

2.4. Infrared Spectrum

Before being dried in a vacuum oven and pulverized, the supramolecular gel was washed with deionized water. The samples were made using a compression method and potassium bromide, and their chemical structure was tested using an infrared spectrometer (Nicolet IS50 FTIR). The infrared scanning region of the supramolecular gel sample was 4000–400 cm^{-1} .

2.5. Thermal Analysis

The supramolecular gel was prepared into powder, and its chemical bonds' thermal stability was characterized using thermal analysis (TAG2, METTLER TOLEDO Company, Greifensee, Switzerland). For measurement, 1 to 2 mg supramolecular gel samples were placed in an airtight saucepan and heated from 25 °C to 1000 °C at 10 °C/min in a nitrogen atmosphere of 50 mL/min.

2.6. Tensile Compression Test

The tensile properties of supramolecular gels were characterized using the CMT4000 electronic universal testing equipment from Shenzhen New Think Material Testing Company, which has a 50 N sensor [34]. Using a cutting tool, the created supramolecular gels were formed into dumbbell-shaped splines with dimensions of 12 mm in length, 2 mm in width, and 2 mm in thickness. The dumbbell-shaped gel splines were coated with a thin coating of silicone oil to prevent water loss during stretching. At a pace of 50 mm/min, uniaxial tensile tests on supramolecular gel splines were conducted to examine the connection between fracture stress (σ) and elongation at break. Formulas (1) and (2) were used to determine the supramolecular gel's tensile stress and strain.

$$\sigma_t = \frac{F_0}{A_0}, \quad (1)$$

In Formula (1): σ_t was the force borne per unit area of the hydrogel sample (MPa); F_0 was the force (N) acting on the hydrogel; A_0 was the cross-sectional area (mm^2) of the initial hydrogel.

$$\varepsilon_t = \frac{\Delta l}{l_0}, \quad (2)$$

In Formula (2): ε_t was the elongation per unit length of hydrogel sample (mm/mm); Δl was the stretch length of hydrogel (mm); l_0 was the initial length (mm) of the hydrogel.

The compression properties of supramolecular gels were tested using an electronic universal testing machine. The compression speed of the supramolecular gel sample was set to 3 mm/min, and the stress–strain curve of the supramolecular gel sample was recorded. The compression stress and strain of supramolecular gel were calculated using Formula (3) and (4) [34].

$$\sigma_c = \frac{F_0}{A_0}, \quad (3)$$

In Formula (3): σ_c defined as compressive stress, which was the force borne per unit area (MPa); F_0 was the force (N) acting on the hydrogel; A_0 was the cross-sectional area (mm^2) of the initial hydrogel.

$$\varepsilon_c = \frac{h_1}{h_0} \times 100\%, \quad (4)$$

In Formula (4): ε_c was the compression ratio per unit length of the hydrogel sample; h_1 was the hydrogel compression shape variable (mm); h_0 was the initial height of the hydrogel (mm).

2.7. Adaptive Filling Ability

The migration and filling state of supramolecular gel in fractures was studied by using a 3D visual fracture physical simulation device (Figure 1). The visual fracture model was mainly made of steel plates and high-pressure borosilicate glass. The specific experimental steps are as follows:

- (a) Inject the supramolecular gel solution into the fracturing model, simulating the formation water in advance;
- (b) Inject deionized water into the fracturing model and seal it; meanwhile, inject saturated simulated drilling fluid into the interior of the visualized fracturing model;
- (c) Apply peripheral pressure to the high-temperature and high-pressure visualization apparatus; meanwhile, apply backpressure to the visualized fracturing model;
- (d) Use a constant-flow pump to alternately inject bridging slurries in an intermediate vessel into the visualized fracturing model;
- (e) Observe the movement pattern of the plugging material in the fracture using a microscopic observation system and back pressure; use a constant-flow pump to inject the bridging plugging slurry in the intermediate container into the visualized fracturing model alternately;
- (f) Observe the advancing state of the supramolecular gel solution in the migrating front of the fracture using a microscopic observation system and image it on the computer to analyze the supramolecular gel's self-adaptive filling ability.

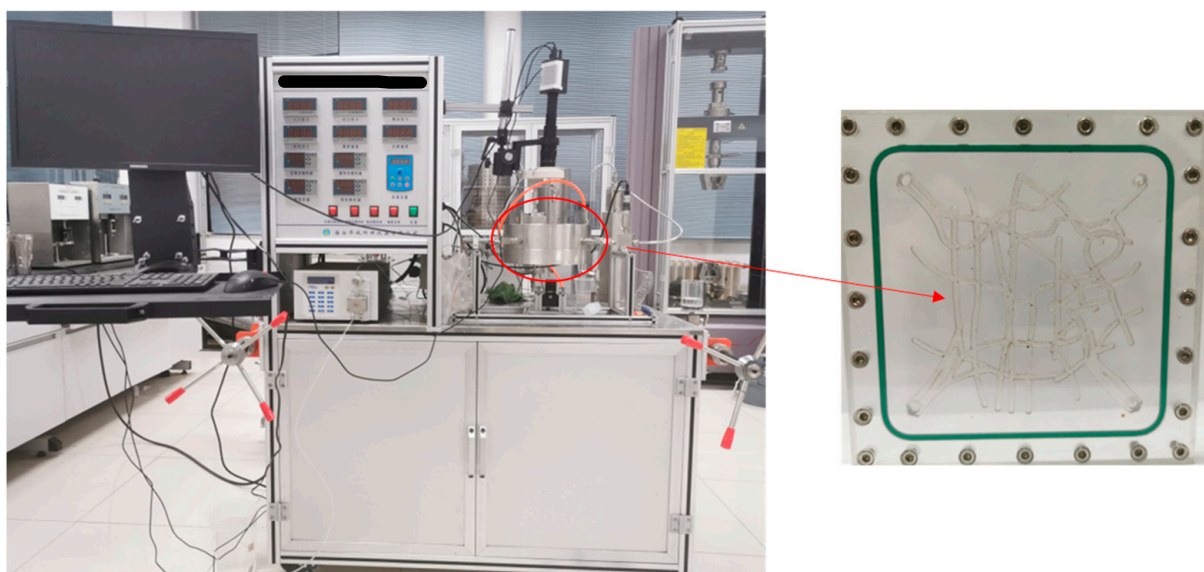


Figure 1. Three-dimensional visual fracture physical simulation device.

3. Results and Discussion

3.1. Preparation and Evaluation of Supramolecular Gels

Typical non-covalent processes for supramolecular synthesis included hydrophobic association and hydrogen bonding. In the present research, hydrogen bonding and hydrophobic association were used as the foundation for the free radical polymerization process used to create supramolecular gels. The gel uses acrylamide as the main chain monomer, 2-acrylamido-2-methylpropanesulfonic acid as a high-temperature resistant monomer, and lauryl methacrylate as a hydrophobic monomer. The reaction structure and synthesis process are shown in Figure 2. Surfactants solubilized hydrophobic monomers

in water to generate micelles in order to achieve the polymerization of hydrophobic and water-soluble monomers. Meanwhile, there were hydrogen bonds and ionic bonds between the carboxyl groups and the copolymers in the structure of sodium alginate. These interactions increase the stability of hydrophobically associating network structures and improve the strength and temperature resistance of supramolecular gels [34].

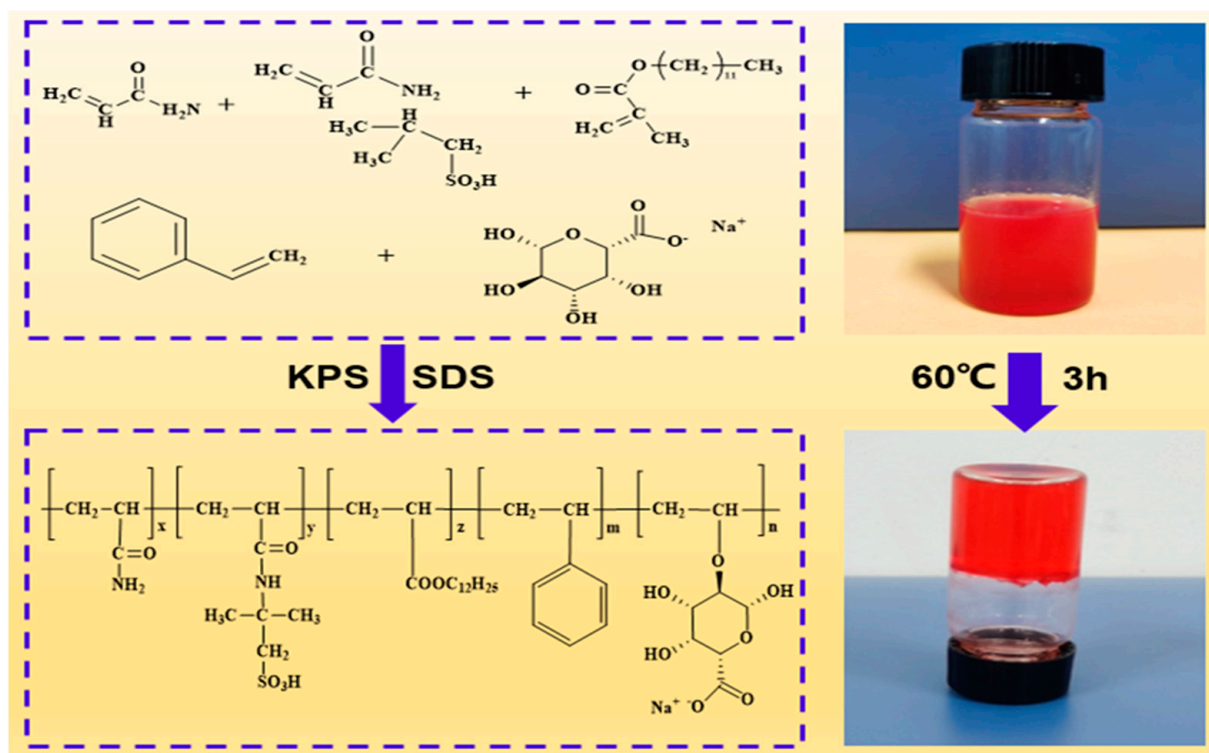


Figure 2. Supramolecular gel reaction structure and synthesis process.

In order to confirm the successful copolymerization of supramolecular gel, infrared spectral scanning, and thermal analysis were performed on supramolecular gel samples. Figure 3a shows that the signal strength is high near the 3196 cm^{-1} . According to the findings, N-H stretching vibrations were present in polyacrylamide, O-H stretching vibrations were present in hydroxyl groups, and O-H stretching vibrations were present in adsorbed water [34]. The 1681.9 cm^{-1} was the characteristic peak of C=O stretching vibration; the signal intensity of the characteristic peak was strong, and the shape of the peak was sharp. The results showed that there were amide groups and carboxylic acid groups, and multimolecular association could easily produce an intermolecular hydrogen bonding effect.

Figure 3b shows that the thermogravimetry of supramolecular gels can be divided into four stages. The first stage was the weight loss caused by evaporation and dehydration of supramolecular gel, and the weight loss rate was 10.9%. In the second stage, the structure of the supramolecular gel sample began to decompose under the action of heat, and the weight loss rate was 19.9%. The third stage was that the chain breaking of supramolecular gel was related to the decomposition of the three-dimensional reticular structure. Weight loss was caused by the ease with which the elements hydrogen and carbon in biological matter were easily volatilized into water vapor and carbon dioxide, respectively. The weight loss rate increased significantly, reaching 39.1%. The fourth stage was the further complete degradation of organic matter in the supramolecular gel structure, and the weight loss rate was 12.8%. Thermogravimetric analysis showed that the supramolecular gel had good thermal stability, the network structure was not easily destroyed, and it had a certain temperature resistance.

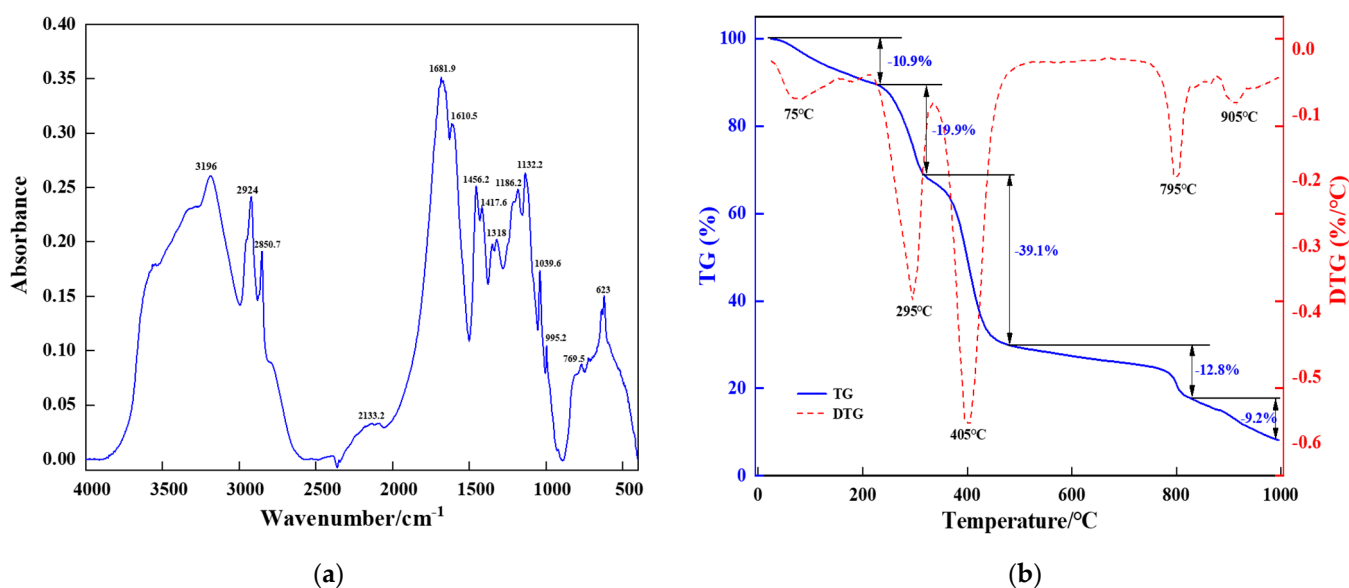


Figure 3. Characterization of the supramolecular gel's structure: (a) infrared spectrum; (b) thermal weight.

3.2. Rheological Properties of Supramolecular Gels

The main parameters characterizing the rheological properties of the gel are viscosity, viscoelasticity, strength, and so on. Among them, elastic modulus and viscous modulus are the key factors affecting the rheological properties of the gel [34]. In order to determine the relationship between the rheology and temperature of supramolecular gel under different stress conditions, the temperature of supramolecular gel samples was scanned at a constant angular frequency ($\omega = 10$ rad/s), and the temperature range was 25–130 °C. The experimental results are shown in Figure 4. When the temperature is 70 °C and $\tau = 100$ Pa, the elastic modulus $G' = 6000$ Pa and the viscous modulus $G'' = 900$ Pa of supramolecular gel; when the temperature is 100 °C and $\tau = 100$ Pa, the elastic modulus $G' = 5000$ Pa and the viscous modulus $G'' = 1000$ Pa of supramolecular gel. When the temperature was lower than 70 °C, the elastic and viscous moduli of the supramolecular gel were stable and fell within the bounds of the linear viscoelastic area. The study demonstrated that the supramolecular gel's three-dimensional network structure skeleton was unaffected by temperature and could sustain exceptional stability in the temperature range. When the temperature is higher than 70 °C, the supramolecular gel's elastic modulus declines, and its viscous modulus rises as the temperature rises. The elastic modulus was often greater than the viscous modulus. This indicated that the supramolecular gel remained elastic throughout the temperature range. Interestingly, the resilience of this elastic state decreased with increasing temperature. Meanwhile, we found that the shear stress also had a certain influence on the elastic and viscous modulus of supramolecular gel, and the influence was greater at low shear stress.

Strain and angular frequency were also the key factors affecting the rheological properties of supramolecular gels. Strain scanning was used to determine the locations of the supramolecular gel's linear viscoelastic area and phase transition point. By using angular frequency scanning, the shear rheological characteristics of supramolecular gels were examined. In this investigation, supramolecular gels were subjected to strain and angular frequency scanning at various temperatures. The experimental results are shown in Figure 5. When the angular frequency was kept constant ($\omega = 10$ rad/s), the supramolecular gel's elastic modulus dropped as the strain rose. When the strain $\gamma = 10\%$, the elastic modulus of the supramolecular gel started to change and dropped sharply. When $T = 140$ °C, $\gamma = 10\%$, the elastic modulus of supramolecular gel $G' = 6900$ Pa, viscous modulus $G'' = 1300$ Pa; when $T = 140$ °C, $\gamma = 100\%$, the elastic modulus of supramolecular gel $G' = 5000$ Pa, viscous modulus $G'' = 1700$ Pa. As a result, fewer than 10% of the supramolecular gel was linearly viscoelastic. When this boundary was crossed, the supramolecular gel started to go through

a gel phase transition, which revealed a change in the elastic and viscous moduli. To determine the effect of angular frequency on the rheological properties of supramolecular gel, the angular frequency scanning of supramolecular gel was performed under constant strain ($\gamma = 1\%$). When $T = 120\text{ }^\circ\text{C}$, $\omega = 20\text{ rad/s}$, the elastic modulus $G' = 20,000\text{ Pa}$, viscous modulus $G'' = 2000\text{ Pa}$ of supramolecular gel; when $T = 120\text{ }^\circ\text{C}$, $\omega = 80\text{ rad/s}$, the elastic modulus $G' = 30,000\text{ Pa}$, viscous modulus $G'' = 2200\text{ Pa}$ of supramolecular gel. The results showed that the elastic modulus of supramolecular gels was positively correlated with the angular frequency. This indicated that the increase in angular frequency could improve the energy storage capacity of the internal network structure of supramolecular gel and maintain good elasticity [34]. The supramolecular gel, meanwhile, revealed a rising elastic modulus trend with rising temperature, indicating that temperature may have an impact on the rheological characteristics of the supramolecular gel.

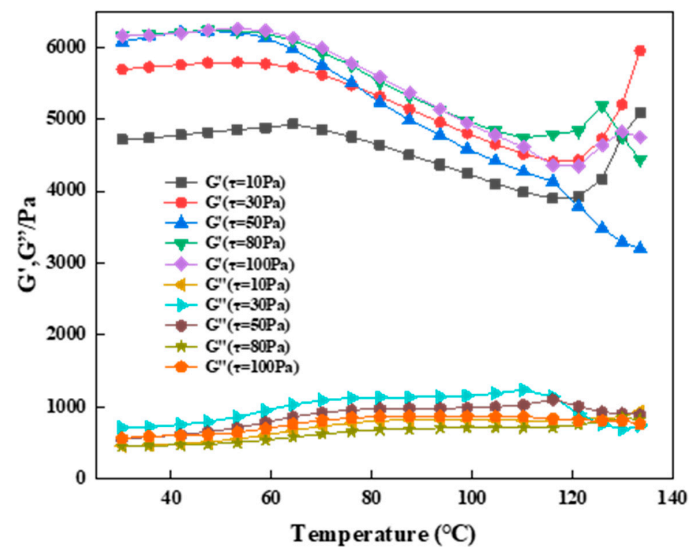


Figure 4. Changes of elastic modulus and viscous modulus of supramolecular gel with temperature under different shear stress at constant angular frequency ($\omega = 10\text{ rad/s}$).

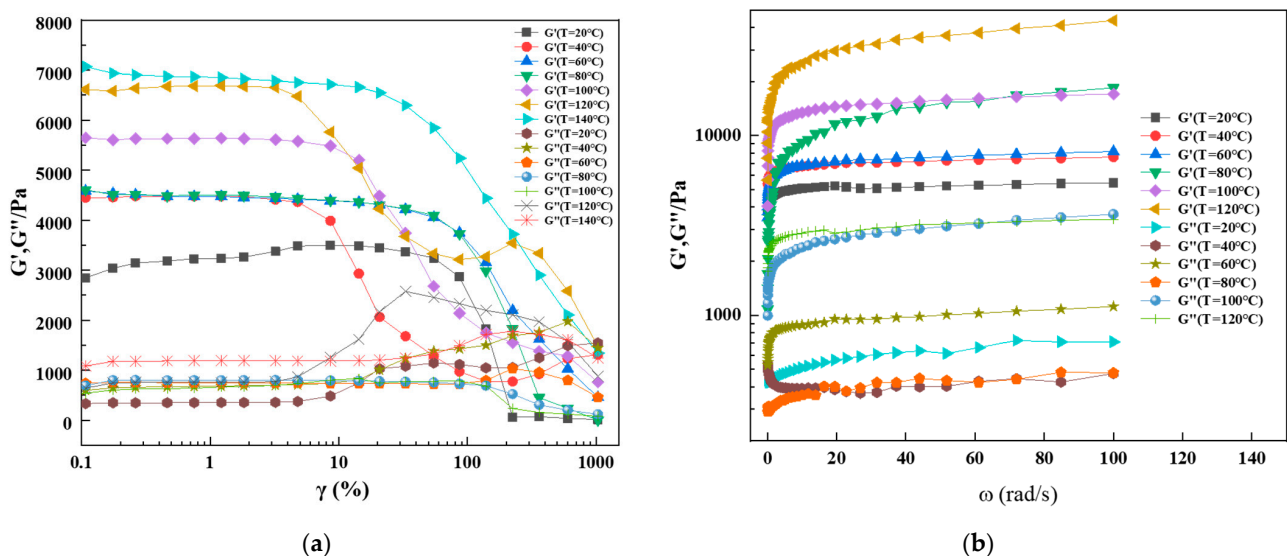


Figure 5. Rheological properties of supramolecular gel at different temperatures: (a) strain scanning of supramolecular gel at different temperatures at a constant angular frequency ($\omega = 10\text{ rad/s}$); (b) angular frequency scanning of supramolecular gel at different temperatures at constant strain ($\gamma = 1\%$).

3.3. Temperature Resistance of Supramolecular Gels

In recent years, polyacrylamide copolymerization systems, HPAM/inorganic delayed cross-linking systems, and HPAM/organic delayed cross-linking systems have been applied successively in oilfields [35]. This greatly improved the problem of poor temperature resistance of polyacrylamide gel. However, the polyacrylamide profile control and plugging agent were not suitable for high-temperature reservoir flooding due to its low plugging rate. Therefore, it must be modified. For example, the introduction of some groups with high-temperature resistance was a common method to improve the temperature and salt resistance of polyacrylamide gel.

Based on hydrogen bonding and hydrophobic interaction, supramolecular gels with good temperature resistance were prepared by introducing high-temperature resistant monomer AMPS. Gel samples in the shape of cylinders were created from the supramolecular gel, which was put into a closed reactor and aged at a high temperature for 72 h in a constant temperature aging furnace at 110 °C, 120 °C, 130 °C and 140 °C, respectively. The samples were taken out, and the microstructure of the supramolecular gel was characterized using scanning electron microscopy (SEM). The microstructure changes of supramolecular gel were observed under high-temperature conditions, and the experimental results are shown in Figures 6 and 7. The outcomes of the experiment demonstrated that despite high-temperature aging, the supramolecular gel could still preserve its original form, its extensibility and tensile properties were good, and it had a certain strength. After curing, the supramolecular gel's microstructure revealed that each layer's networks were intricately interconnected, had a dense three-dimensional network structure, and had impressive temperature tolerance.

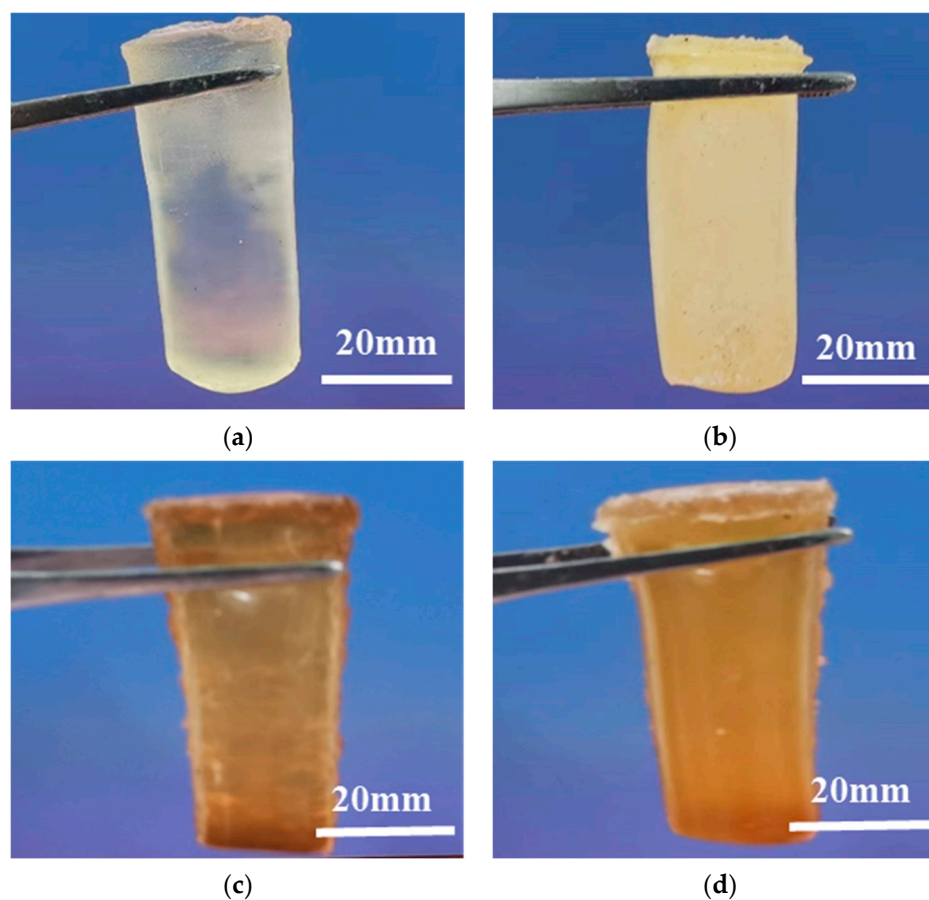


Figure 6. After being heated to a high temperature, supramolecular gel's physical appearance: (a) 110 °C; (b) 120 °C; (c) 130 °C; (d) 140 °C.

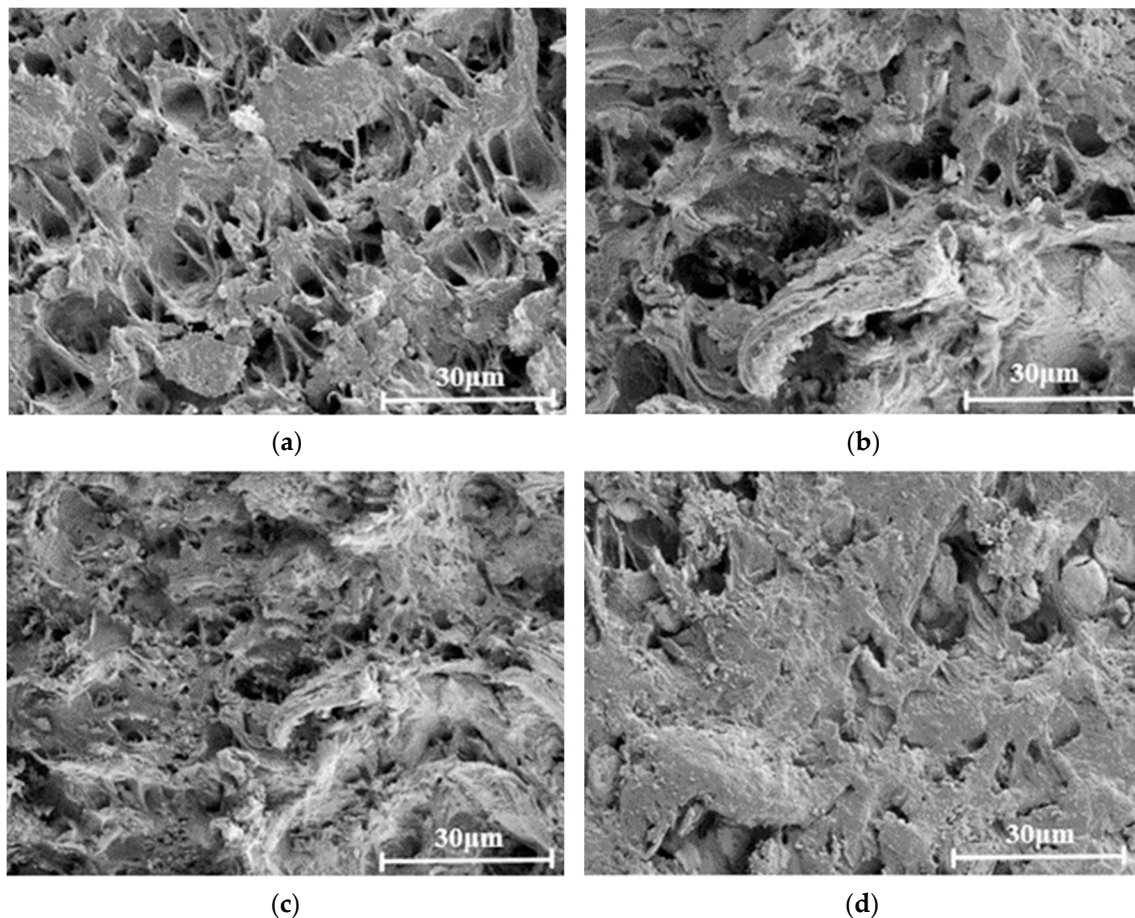


Figure 7. SEM image of supramolecular gel aged at high temperature: (a) 110 °C; (b) 120 °C; (c) 130 °C; (d) 140 °C.

In this experiment, under constant strain ($\gamma = 1\%$) and angular frequency ($\omega = 10$ rad/s), supramolecular gels curing at high temperatures were examined for their rheological characteristics, and their high-temperature resistance was further determined. The relationship between elastic modulus, viscous modulus, and temperature stability of supramolecular gels is shown in Figure 8. Under the situation of continuous strain ($\gamma = 1\%$), the elastic and viscous moduli of supramolecular gel initially increase and subsequently tend to stabilize with increasing angular frequency. When $T = 140$ °C, $\omega = 20$ rad/s, the elastic modulus $G' = 103,000$ Pa and viscous modulus $G'' = 20,000$ Pa of supramolecular gel; when $T = 140$ °C, $\omega = 80$ rad/s, the elastic modulus $G' = 104,000$ Pa and viscous modulus $G'' = 26,000$ Pa of supramolecular gel. Additionally, the elastic and viscous moduli increase with temperature. Under the condition of constant angular frequency ($\omega = 10$ rad/s), When $T = 140$ °C, $\gamma = 10\%$, the elastic modulus $G' = 7000$ Pa and viscous modulus $G'' = 1700$ Pa of supramolecular gel; when $T = 140$ °C, $\gamma = 100\%$, the elastic modulus $G' = 6500$ Pa and viscous modulus $G'' = 1800$ Pa of supramolecular gel. Therefore, the elastic modulus of supramolecular gel was stable at first and then decreased with the increase in strain. This indicated that the increase in strain had a certain weakening effect on the rheological properties of supramolecular gel and reduced the elastic modulus and temperature resistance of supramolecular gel to a certain extent. Compared with the cross-linked gel synthesized by Islamov et al. [36], which showed better rheological properties at a high temperature of 90 °C, our supramolecular gel aged at 110 °C to 140 °C has higher temperature resistance and more substantial mechanical properties.

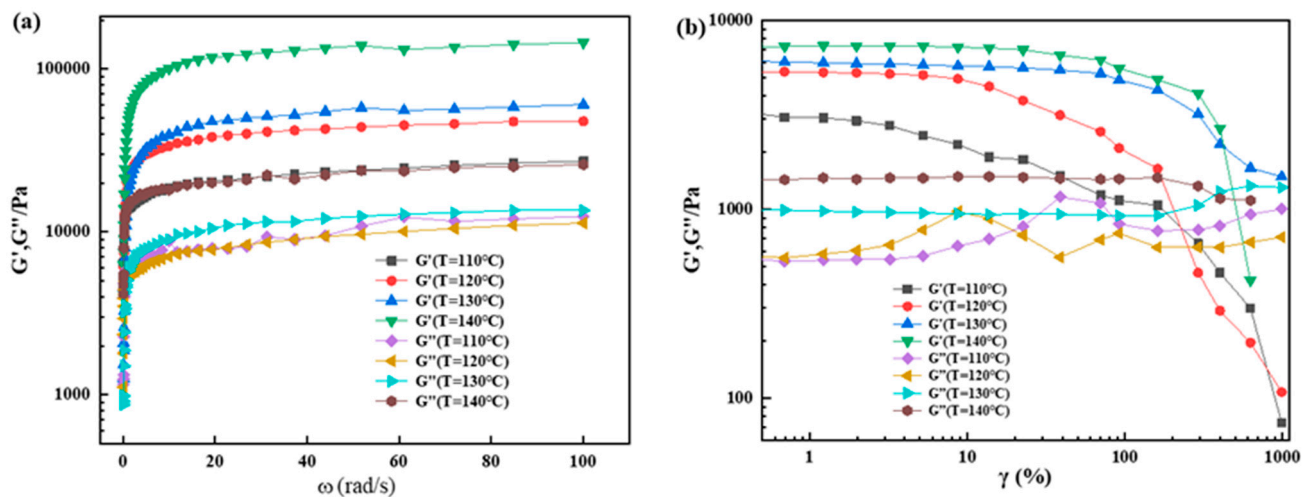


Figure 8. Rheological properties of supramolecular gel after curing at different temperatures: (a) Constant strain ($\gamma = 1\%$) angular frequency change; (b) Constant angular frequency ($\omega = 10$ rad/s), strain variation.

3.4. Mechanical Properties of Supramolecular Gels

In the research of improving the mechanical properties of gels, many hydrogels with high strength have been synthesized and prepared. These include double network structure hydrogels, nano hybrid hydrogels, and sliding ring hydrogels [37]. In order to characterize the mechanical strength of these gels, unidirectional tensile tests, stress relaxation tests, indentation tests, and fundamental frequency tests are usually used. The tensile test could reveal the stress–strain relationship of materials under static load and the common characteristics and basic laws of elastic deformation, plastic deformation, and fracture [38]. It could also evaluate the basic mechanical properties of materials, such as yield strength, tensile strength, elongation, and section shrinkage. Figure 9 shows the results of the uniaxial tensile test of supramolecular gel samples. The study showed that when the elongation of supramolecular gel reaches 300%, the tensile stress is 2.33 MPa. The supramolecular gel sample was stretched for a second time after recovering the deformation, and the tensile stress could still reach 1.17 MPa when the stretching elongation was 200%. These findings suggested that supramolecular gel exhibited high deformation recovery during cyclic stretching as well as outstanding tensile mechanical properties.

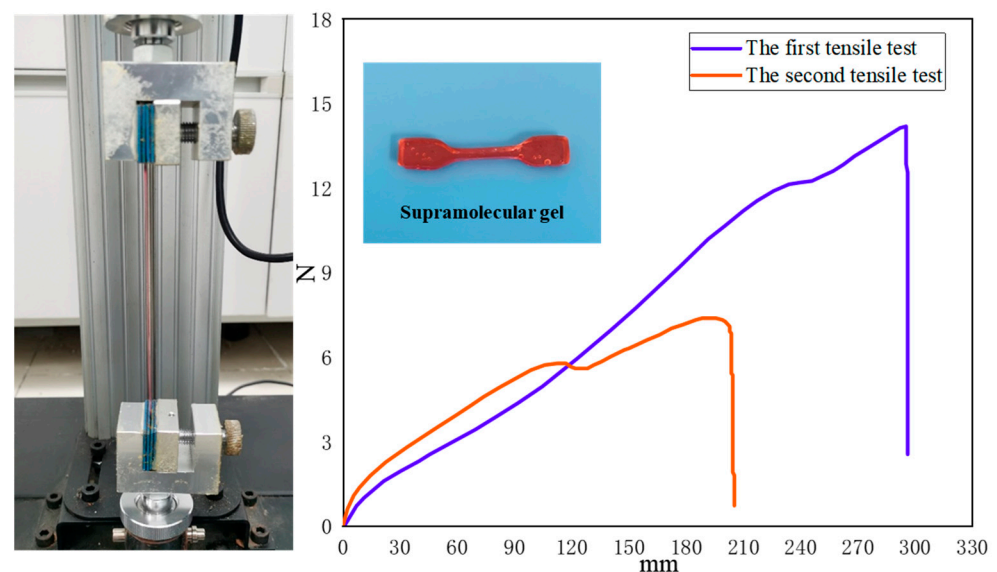


Figure 9. Tensile results of supramolecular gel.

Supramolecular gel samples were prepared into cylinders to study their compression properties. The diameter of the sample was 20 mm, and the height was 8 mm. The compression test results of samples of supramolecular gel were displayed in Figure 10 at room temperature. The outcomes demonstrated that following compression deformation, the supramolecular gel could maintain good elastic deformation properties and swiftly revert to its initial state. Meanwhile, according to Formulas (3) and (4), the compression stress of supramolecular gel could reach 4.78 MPa when the compression ratio was 91.2%. The results showed that supramolecular gel had excellent compression resistance and could improve its compression strength by dissipating energy via various hydrogen bonds in its three-dimensional network structure.

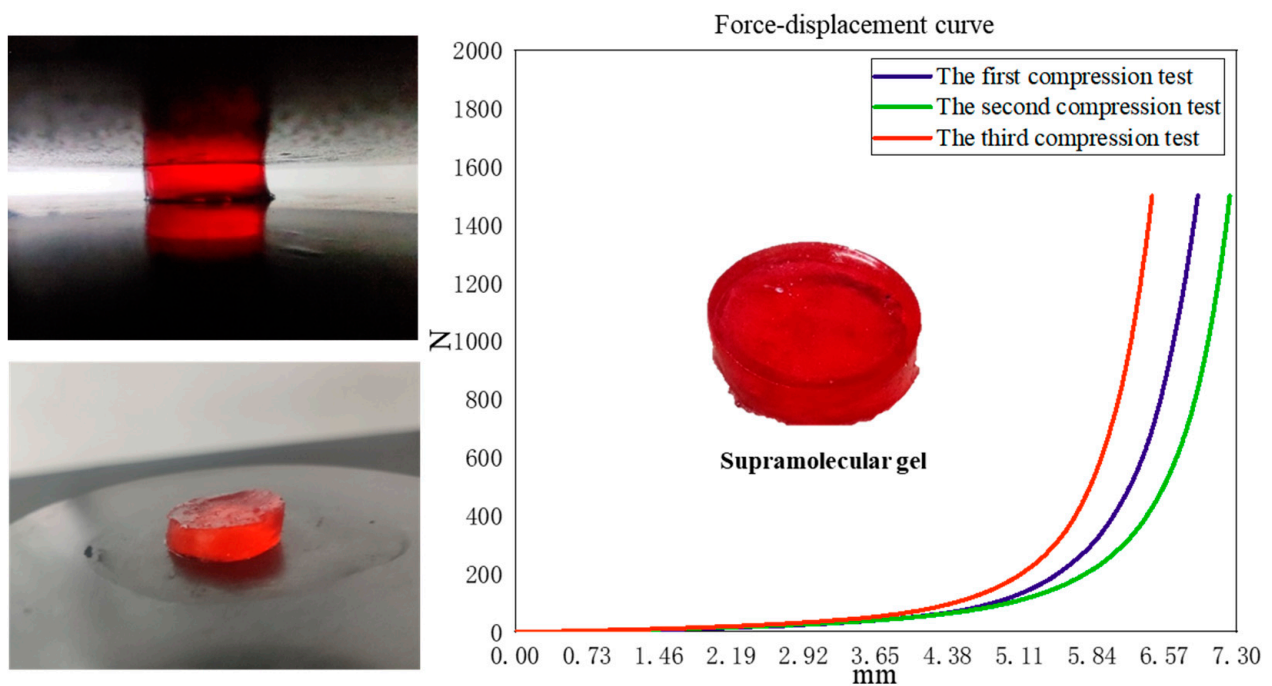


Figure 10. Compression results of supramolecular gel.

3.5. Adaptive Filling and Plugging Performance of Supramolecular Gel

For the formation with strong reservoir heterogeneity and unpredictability of reservoir pore size, the particle size of conventional plugging materials cannot be strictly consistent with the pore size [39]. The adaptive gel was not affected by the fracture size and could adjust its shape to plug holes of different shapes. The use of adaptive gel did not need to predict the aperture of the fractured formation in advance, which could adaptively plug the pore of rock surface in a large range and could plug the lost layer with a wide aperture distribution quickly. The filter layer formed after plugging was thin, which would not affect the drilling construction while preventing and plugging the oil layer.

According to the adaptive filling effect of supramolecular gel in the fracture shown in Figure 11, it could form a cross-linked and wound high-toughness gel network structure via non-covalent interaction after supramolecular gel entered the fracture. The gel particles were piled and adsorbed in the fracture pores, and by extrusion deformation and water absorption expansion, the overall compact supramolecular gel plugging layer was created. Meanwhile, the intelligent plugging drilling fluid prepared with supramolecular gel material could quickly form a fine barrier layer on the rock surface of the reservoir. Effectively isolate the drilling fluid into the reservoir and reduce the adverse effects, such as the decrease in permeability caused by the drilling fluid entering the reservoir, so as to achieve the purpose of protecting the reservoir.

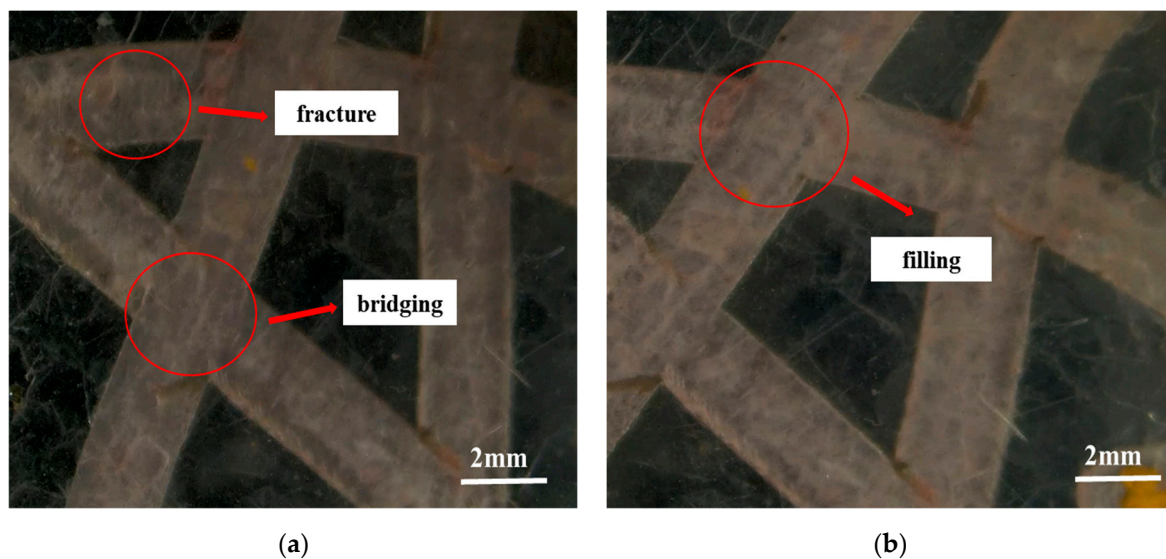


Figure 11. Adaptive filling effect of supramolecular gel in fractures: (a) supramolecular gel entered the stage of fracture bridging accumulation; (b) supramolecular gel formed an integral plugging layer in the fracture.

Supramolecular gels belong to the category of adaptive gels, which can show excellent plugging effects on complex loss layers with different fracture apertures. The plugging success rate could reach more than 90%, and the pressure-bearing capacity of the gel plugging layer could reach up to 6.3 MPa. Meanwhile, the smart plugging fluid prepared with supramolecular gel materials could quickly accumulate to form a tight gel slug on the rock fracture surface of the reservoir via external forces (Figure 12). The gel plugging layer could effectively prevent drilling fluid from entering the reservoir and reduce the adverse effects, such as permeability reduction caused by drilling fluid entering the reservoir. The supramolecular gel plugging layer had the purpose of protecting the reservoir to a certain extent.

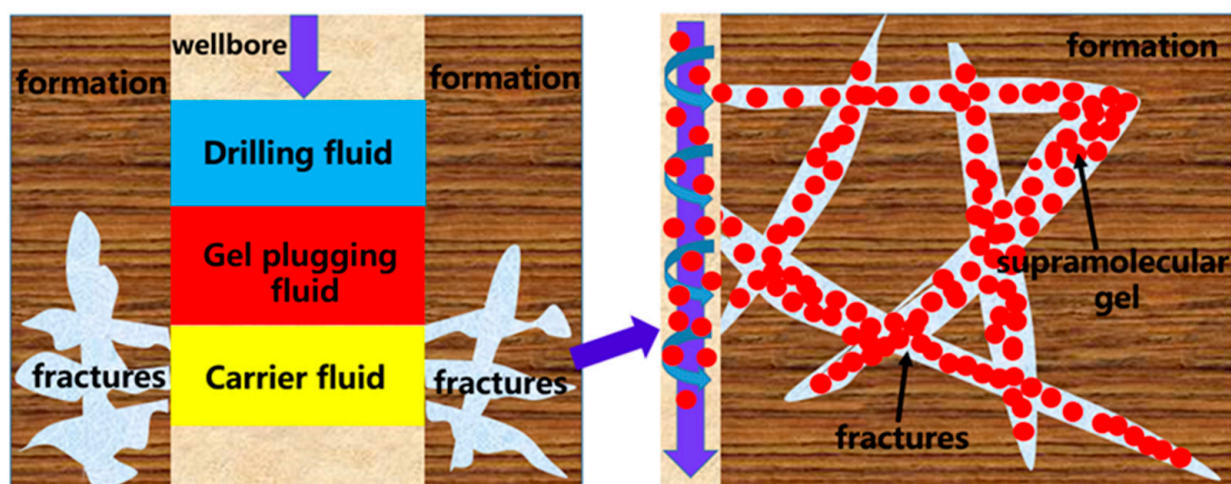


Figure 12. Schematic diagram of supramolecular gel adaptive filling and plugging.

4. Conclusions

- (1) The supramolecular gel created in this work has exceptional rheological qualities based on non-covalent interactions such as hydrophobic association and hydrogen bonding. When the strain was less than 10%, the supramolecular gel displayed a nice linear viscoelastic area. The increase in strain weakens the rheological properties

of supramolecular gel and reduces the elastic modulus of supramolecular gel to a certain extent.

- (2) The supramolecular gel maintained its original main body shape even after being aged at high temperatures and possessed a dense, stable, three-dimensional network structure. The networks of supramolecular gels were closely connected with each other, their stretching properties were good, and they had excellent temperature resistance and mechanical strength.
- (3) (Supramolecular gels had excellent tensile and compression properties and had good deformation recovery properties after cyclic tension and compression. When the elongation of the supramolecular gel reached 300%, the tensile stress was 2.33 MPa. When the compression ratio of supramolecular gel was 91.2%, the compression stress of supramolecular gel could reach 4.78 MPa.
- (4) Supramolecular gel not only had excellent anti-leakage and plugging ability but also could significantly improve the pressure-bearing ability of the formation. The supramolecular gel could show an excellent plugging effect on the complex loose layer with different pore sizes, the plugging success rate could reach more than 90%, and the plugging layer could withstand the external pressure of 6.3 MPa.
- (5) The intelligent plugging drilling fluid prepared with supramolecular gel material could quickly form a fine barrier layer on the surface of reservoir rock. It could effectively isolate the drilling fluid from entering the reservoir and reduce the adverse effects, such as the decrease in permeability caused by the drilling fluid entering the reservoir, so as to achieve the purpose of protecting the reservoir.

Author Contributions: Conceptualization, X.D.: Investigation, Data Analysis, Writing. Y.B.: Supervision, Methodology, Investigation, Funding Acquisition. S.F.: Resources, Data Analysis. H.L.: Investigation, Resources. Z.L.: Investigation, Resources. All authors have read and agreed to the published version of the manuscript.

Funding: This study was funded by the Key Science and Technology Projects of Tarim Oilfield (Grant 201021102443).

Data Availability Statement: Data is contained within the article.

Conflicts of Interest: The authors declare that they have no known competing financial interests or personal relationships that could have appeared to influence the work reported in this paper.

References

1. Jiang, L.; Liu, Z.W.; Liu, J.; He, S.; Wu, X.; Shao, W. Supramolecular lignin-containing hydrogel for flexible strain sensor via host-guest interaction and dynamic redox system. *Ind. Crops Prod.* **2023**, *192*, 116083. [[CrossRef](#)]
2. Yu, D.; Teng, Y.; Zhou, N.; Xu, Y.; Wang, X.; Lin, X.; Wang, Q.L.; Xue, C. A Low-modulus, Adhesive, and Highly Transparent Hydrogel for Multi-use Flexible Wearable Sensors. *Colloids Surf. A Physicochem. Eng. Asp.* **2022**, *659*, 130752. [[CrossRef](#)]
3. Mohammadinezhad, A.; Marandi, G.B.; Farsadrooh, M.; Javadian, H. Synthesis of poly(acrylamide-co-itaconic acid)/MWCNTs superabsorbent hydrogel nanocomposite by ultrasound-assisted technique: Swelling behavior and Pb (II) adsorption capacity. *Ultrason. Sonochemistry* **2018**, *49*, 1–12. [[CrossRef](#)] [[PubMed](#)]
4. Wang, X.; Lu, H.; Wu, N.; Hui, D.; Fu, Y. Unraveling bio-inspired pre-swollen effects of tetra-polyethylene glycol double network hydrogels with ultra-stretchable yielding strain. *Smart Mater. Struct.* **2019**, *28*, 035005. [[CrossRef](#)]
5. Nie, Z.; Peng, K.; Lin, L.; Yang, J.; Cheng, Z.; Gan, Q.; Chen, Y.; Feng, C. A conductive hydrogel based on nature polymer agar with self-healing ability and stretchability for flexible sensors. *Chem. Eng. J.* **2023**, *454*, 139843. [[CrossRef](#)]
6. Zhao, D.; Feng, M.; Zhang, L.; He, B.; Chen, X.; Sun, J. Facile synthesis of self-healing and layered sodium alginate/polyacrylamide hydrogel promoted by dynamic hydrogen bond. *Carbohydr. Polym.* **2021**, *256*, 117580. [[CrossRef](#)]
7. Zhu, Y.; Luo, Q.; Zhang, H.; Cai, Q.; Li, X.; Shen, Z.; Zhu, W. A shear-thinning electrostatic hydrogel with antibacterial activity by nanoengineering of polyelectrolytes. *Biomater. Sci.* **2020**, *8*, 1394–1404. [[CrossRef](#)]
8. Yang, Y.; Liu, S.; Cai, X.; Ma, D.; Xu, J. Supramolecular hydrogel containing multi-generation poly(L-lysine) dendrons for sustained co-delivery of docetaxel and matrix metalloproteinase-9 short hairpin RNA plasmid. *J. Bioact. Compat. Polym.* **2019**, *35*, 3–23. [[CrossRef](#)]
9. Kesmez, Ö. Preparation of hybrid nanocomposite coatings via sol-gel method for hydrophobic and self-cleaning properties. *J. Mol. Struct.* **2020**, *1205*, 127572. [[CrossRef](#)]

10. Chang, K.; Chen, W.; Chen, C.; Ko, C.; Liu, S.; Chen, J. Chemical cross-linking on gelatin-hyaluronan loaded with hinokitiol for the preparation of guided tissue regeneration hydrogel membranes with antibacterial and biocompatible properties. *Mater. Sci. Eng. C* **2021**, *119*, 111576. [[CrossRef](#)]
11. Fan, X.; Geng, J.; Wang, Y.; Gu, H. PVA/gelatin/ β -CD-based rapid self-healing supramolecular dual-network conductive hydrogel as bidirectional strain sensor. *Polymer* **2022**, *246*, 124769. [[CrossRef](#)]
12. Wang, R.; Li, N.; Zhang, L.; Gao, L.; Hong, W.; Jiao, T. Facile Construction of Gelatin/Polyacrylamide Acrylic Acid/Sodium Alginate-Based Triple-Network Composite Hydrogels with Excellent Mechanical Performances. *Integr. Ferroelectr.* **2022**, *227*, 98–109. [[CrossRef](#)]
13. Chen, Z.; Tang, J.; Zhang, N.; Chen, Y.; Chen, Y.; Li, H.; Liu, H. Dual-network sodium alginate/polyacrylamide/laponite nanocomposite hydrogels with high toughness and cyclic mechano-responsiveness. *Colloids Surf. A Physicochem. Eng. Asp.* **2022**, *633*, 127867. [[CrossRef](#)]
14. Chen, Q.; Yan, X.; Zhu, L.; Chen, H.; Jiang, B.H.; Wei, D.; Huang, L.; Yang, J.; Liu, B.; Zheng, J. Improvement of Mechanical Strength and Fatigue Resistance of Double Network Hydrogels by Ionic Coordination Interactions. *Chem. Mater.* **2016**, *28*, 5710–5720. [[CrossRef](#)]
15. Guo, X.; Lu, Y.; Fu, D.; Yu, C.; Yang, X.; Zhong, W. Ultrahigh ionic conductivity and alkaline tolerance of poly(amidoxime)-based hydrogel for high performance piezoresistive sensor. *Chem. Eng. J.* **2023**, *452*, 139208. [[CrossRef](#)]
16. Li, S.; Bu, X.; Wu, L.; Ma, X.; Diao, W.; Zhuang, Z.; Zhou, Y. Tough and recoverable triple-network hydrogels based on multiple pairs of toughing mechanisms with excellent ionic conductivity as stable strain sensors. *Polym. Eng. Sci.* **2019**, *59*, 1657–1666. [[CrossRef](#)]
17. Qin, M.; Guo, Y.; Su, F.; Huang, X.; Qian, Q.; Zhou, Y.; Pan, J. High-strength, fatigue-resistant, and fast self-healing antibacterial nanocomposite hydrogels for wound healing. *Chem. Eng. J.* **2022**, *455*, 140854. [[CrossRef](#)]
18. Liu, J.; Zhang, Z.; Liu, Z.; Yu, Y. Preparation of a nanocomposite hydrogel with high adhesion, toughness, and inherent antibacterial properties by a one-pot method. *Colloids Surf. A Physicochem. Eng. Asp.* **2023**, *656*, 130368. [[CrossRef](#)]
19. Jia, H.J.; Yang, X.; Sanxi, L.; Yu, P.; Zhang, J. Nanocomposite gel of high-strength and degradability for temporary plugging in ultralow-pressure fracture reservoirs. *Colloids Surf. A Physicochem. Eng. Asp.* **2020**, *585*, 124108. [[CrossRef](#)]
20. Gu, H.; Zhang, H.; Ma, C.; Sun, H.; Liu, C.; Dai, K.; Zhang, J.; Wei, R.; Ding, T.; Guo, Z. Smart strain sensing organic–inorganic hybrid hydrogels with nano barium ferrite as the cross-linker. *J. Mater. Chem. C* **2019**, *7*, 2353–2360. [[CrossRef](#)]
21. Ling, H.; Shen, Y.; Xu, L.; Pan, H.; Shen, N.; Li, K.; Ni, K. Preparation and characterization of dual-network interpenetrating structure hydrogels with shape memory and self-healing properties. *Colloids Surf. A Physicochem. Eng. Asp.* **2022**, *636*, 128061. [[CrossRef](#)]
22. Haldhar, R.; Parveen Asrafali, S.; Jayprakash Raorane, C.; Periyasamy, T.; Kim, S. Performance of cross-linked polymers as a potential anticorrosive coating for low carbon steel in acidic condition: Experimental and computational studies. *J. Mol. Liq.* **2022**, *360*, 119384. [[CrossRef](#)]
23. Wahid, F.; Hu, X.; Chu, L.; Jia, S.; Xie, Y.; Zhong, C. Development of bacterial cellulose/chitosan based semi-interpenetrating hydrogels with improved mechanical and antibacterial properties. *Int. J. Biol. Macromol.* **2019**, *122*, 380–387. [[CrossRef](#)] [[PubMed](#)]
24. Zhu, T.; Cheng, Y.; Cao, C.; Mao, J.; Li, L.; Huang, J.; Gao, S.; Dong, X.; Chen, Z.; Lai, Y. A semi-interpenetrating network ionic hydrogel for strain sensing with high sensitivity, large strain range, and stable cycle performance. *Chem. Eng. J.* **2020**, *385*, 123912. [[CrossRef](#)]
25. Bai, Y.; Zhang, Q.; Sun, J.; Jiang, G.; Lv, K. Double network self-healing hydrogel based on hydrophobic association and ionic bond for formation plugging. *Pet. Sci.* **2022**, *19*, 2150–2164. [[CrossRef](#)]
26. Tuncaboylu, D.C.; Sari, M.; Oppermann, W.P.; Okay, O. Tough and Self-Healing Hydrogels Formed via Hydrophobic Interactions. *Macromolecules* **2011**, *44*, 4997–5005. [[CrossRef](#)]
27. Chen, X.; Sun, P.; Liu, H. Crosslinked Gels Containing Hydrophobic Ionic Liquids towards Reliable Sensing Applications. *Chin. J. Polym. Sci.* **2020**, *38*, 332–341. [[CrossRef](#)]
28. Wang, Y.; Xiong, J.; Peng, F.; Li, Q.; Zeng, M. Building a supramolecular gel with an ultra-low-molecular-weight Schiff base gelator and its multiple-stimulus responsive properties. *Colloids Surf. A Physicochem. Eng. Asp.* **2022**, *640*, 128445. [[CrossRef](#)]
29. Sun, H.; Jiang, J.; Zhang, L.; Yuan, C.; Jiang, Y.; Liu, P. Rheological and atomization behavior of glycyrrhizic acid based supramolecular gel propellant simulant. *Colloids Surf. A Physicochem. Eng. Asp.* **2022**, *640*, 128460. [[CrossRef](#)]
30. Huang, X.; Meng, X.; Li, M.; Sun, J.; Lv, K.; Gao, C. Improving the Weak Gel Structure of an Oil-Based Drilling Fluid by Using a Polyamide Wax. *Gels* **2022**, *8*, 631. [[CrossRef](#)]
31. Sun, J.; Yingrui, B.; Cheng, R.; Kaihe, L.; Liu, F.; Jie, F.; Lei, S.; Zhang, J.; Huijun, H. Research progress and prospect of plugging technologies for fractured formation with severe lost circulation. *Pet. Explor. Dev.* **2021**, *48*, 732–743. [[CrossRef](#)]
32. Durán-Valencia, C.; Bai, B.; Reyes, H.; Fajardo-Lopez, R.; Barragán-Aroche, F.; López-Ramírez, S. Development of enhanced nanocomposite preformed particle gels for conformance control in high-temperature and high-salinity oil reservoirs. *Polym. J.* **2014**, *46*, 277–284. [[CrossRef](#)]
33. Jiang, Q.; Jiang, G.; Wang, C.; Lili, Y.; Ren, Y.; Liu, P.; Yawei, S. The influence of fiber on the rheological properties, microstructure and suspension behavior of the supramolecular viscoelastic fracturing fluid. *J. Nat. Gas Sci. Eng.* **2016**, *35*, 1207–1215. [[CrossRef](#)]
34. Yang, J.; Sun, J.; Bai, Y.; Lv, K.; Li, J.Y.; Li, M.; Zhu, Y. Preparation and characterization of supramolecular gel suitable for fractured formations. *Pet. Sci.* **2023**, *20*, 2324–2342. [[CrossRef](#)]

35. Wu, W.; Hou, J.; Qu, M.; Yang, Y.; Zhang, W.; Wu, W.; Wen, Y.; Liang, T.; Xiao, L. A novel polymer gel with high-temperature and high-salinity resistance for conformance control in carbonate reservoirs. *Pet. Sci.* **2022**, *19*, 3159–3170. [[CrossRef](#)]
36. Islamov, S.; Bondarenko, A.V.; Gabibov, A.F.; Mardashov, D. Polymer compositions for well killing operation in fractured reservoirs. In *Advances in Raw Material Industries for Sustainable Development Goals*; CRC Press: Boca Raton, FL, USA, 2020.
37. Wang, R.; Ma, Y.; Chen, P.; Sun, L.; Liu, Y.; Gao, C. A double network conductive gel with robust mechanical properties based on polymerizable deep eutectic solvent. *Colloids Surf. A Physicochem. Eng. Asp.* **2023**, *656*, 130349. [[CrossRef](#)]
38. Ciftbudak, S.; Orakdogan, N. Enhanced sustained responsive-systems based on anionically modified gelatin-containing hybrid gels: A route to correlate physico-mechanical and swelling properties. *Colloids Surf. A Physicochem. Eng. Asp.* **2022**, *651*, 129756. [[CrossRef](#)]
39. Lei, S.F.; Sun, J.S.; Bai, Y.R.; Lv, K.H.; Zhang, S.P.; Liu, F.; Zhang, J. Plugging performance and mechanism of temperature-responsive adhesive lost circulation material. *J. Pet. Sci. Eng.* **2022**, *217*, 110771. [[CrossRef](#)]

Disclaimer/Publisher's Note: The statements, opinions and data contained in all publications are solely those of the individual author(s) and contributor(s) and not of MDPI and/or the editor(s). MDPI and/or the editor(s) disclaim responsibility for any injury to people or property resulting from any ideas, methods, instructions or products referred to in the content.